

## Supporting Information

### Enhancing solar steam generation through manipulating the heterostructure of PVDF membranes with reduced reflection and conduction

Tiantian Li<sup>a,b</sup>, Qile Fang<sup>a,b</sup>, Haibo Lin<sup>a</sup> and Fu Liu<sup>a,b\*</sup>

a: Key laboratory of Marine Materials and Related Technologies, Ningbo Institute of Materials Technology & Engineering, Chinese Academy of Sciences, No. 1219 Zhongguan West Rd, Ningbo, 315201, China

b: University of Chinese Academy of Sciences, 19 A Yuquan Rd, Shijingshan District, Beijing, 100049, China

\*Please address correspondences to:

Prof. Fu Liu

Address: Ningbo Institute of Materials Technology & Engineering, Chinese Academy of Sciences, No. 1219 Zhongguan West Rd, Ningbo, 315201, China

Tel.: +8657486325963;

Fax: +8657486325963;

E-mail: fu.liu@nimte.ac.cn

Samples, immersing in the mixed coagulation bath for 1 min, 3 min and 5 min, were used to investigate the structure composition of heterostructured membrane via salt induced phase separation. From **Figure S1**, the morphologies of top surfaces of heterostructured membrane changed obviously with the prolongation of the immersion time of the membrane in the salt mediated coagulation bath. The spherical structure on the surface for membrane in coagulation bath for 1 min didn't have enough time to grow, resulting in porosity of top surface smaller than that of other membranes. For the bottom surface as exhibited in **Figure S2**, the bottom morphologies of all membranes in this paper was the same with flower-like structures. The reason was that the delayed phase transformation was beneficial for the growth of structure especially for the bottom surface. On the other hand, without the enrichment of sodium chloride in the lower surface, the structures can grow into flower-like with micro/nano structures which were conducive to the hydrophobicity.

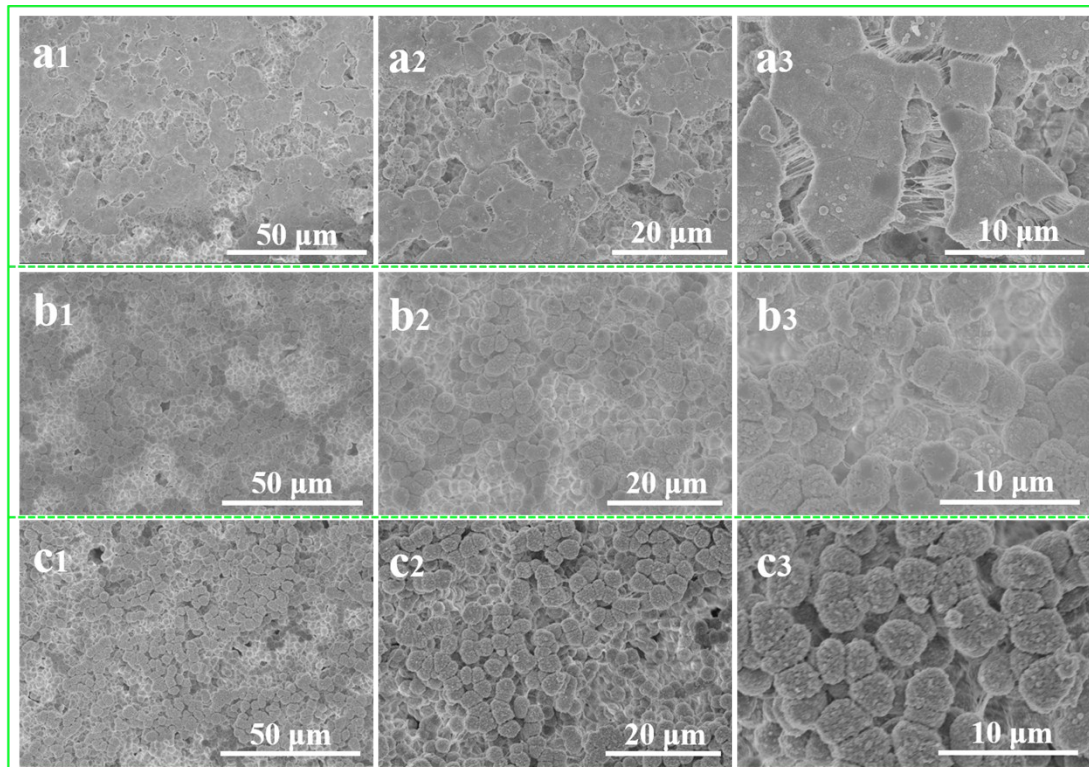


**Figure S1.** Top surface morphologies with different magnifications of heterostructured membranes with different immersion time in the salt mediated coagulation bath: (a<sub>1</sub>, a<sub>2</sub>, a<sub>3</sub>) 1min; (b<sub>1</sub>, b<sub>2</sub>, b<sub>3</sub>) 3min; (c<sub>1</sub>, c<sub>2</sub>, c<sub>3</sub>) 5min.

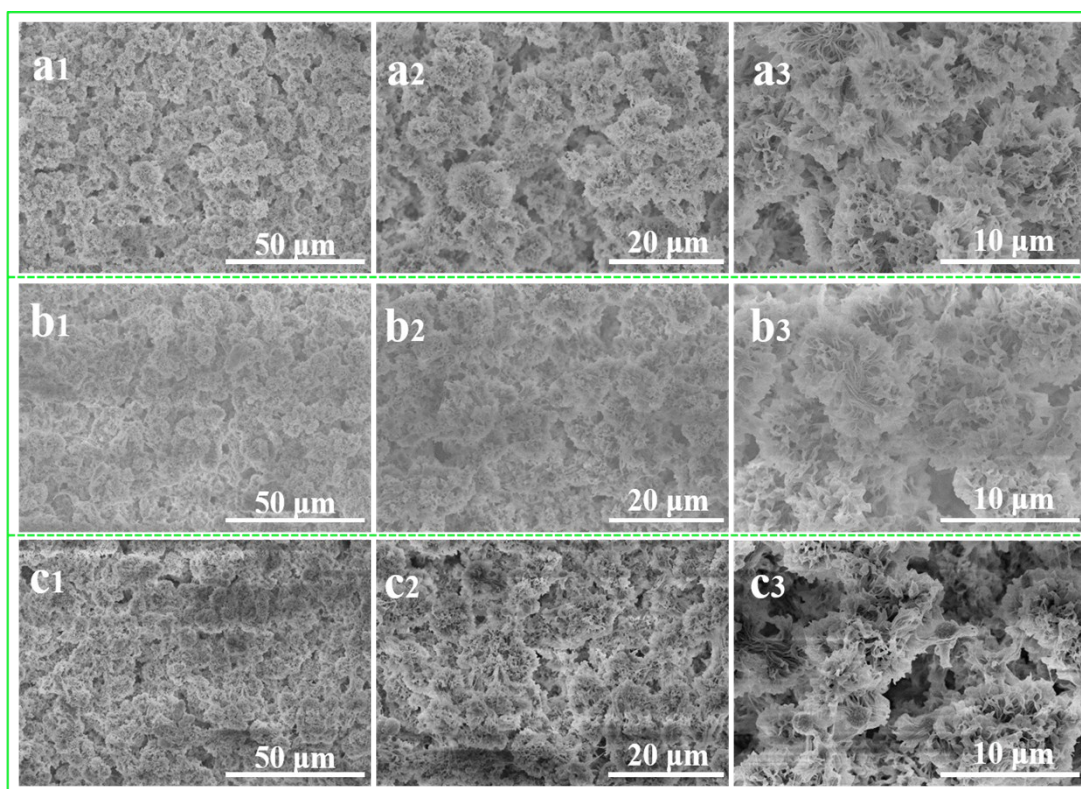


**Figure S2.** The bottom surface morphologies with different magnifications of heterostructured membranes with different immersion time in the salt mediated coagulation bath: (a<sub>1</sub>, a<sub>2</sub>, a<sub>3</sub>) 1min; (b<sub>1</sub>, b<sub>2</sub>, b<sub>3</sub>) 3min; (c<sub>1</sub>, c<sub>2</sub>, c<sub>3</sub>) 5min.

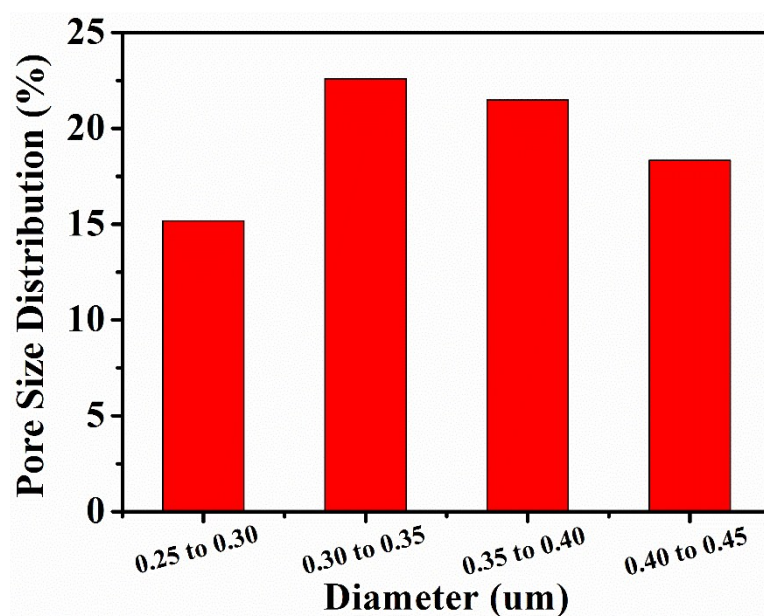


**Figure S3.** The pore size distribution of the heterostructured membrane. The average pore size is 0.36 μm.

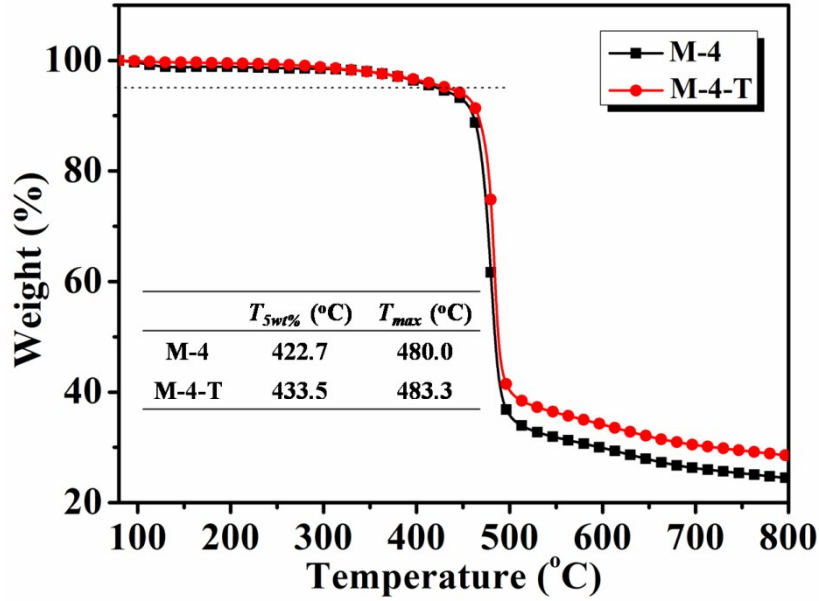


**Figure S4.** TGA curves of M-4 and M-4-T in nitrogen.

It can be seen from **Figure S5** that the thickness of hydrophilic spherical structure in heterostructured membrane increased with the prolongation of soaking time in mixed coagulation bath, and the thickness of spherical structure was basically unchanged after 3 min. More hydrophilic copolymer will segregate into the top layer with extending immersion time. The delayed phase transformation occurred in the mixed coagulation bath, which would cause the membrane to solidify slowly.<sup>1</sup> Meanwhile, the sodium chloride entered the interior of the membrane with the exchange of solvent and non-solvent to form nucleating points of the PVDF chains, which was beneficial to the formation of spherical particles. The thickness of the hydrophilic layer increased as the soaking time in the coagulation bath increased. The thickness of hydrophilic layer was 95.84  $\mu\text{m}$  for M-1 while it was 144.84  $\mu\text{m}$  for M-2. After 3 min, the membrane was completely solidified and the chains of PVDF can't move any more. Therefore, the thicknesses of hydrophilic layer for samples immersed in coagulation bath for 3 min or longer were almost constant.

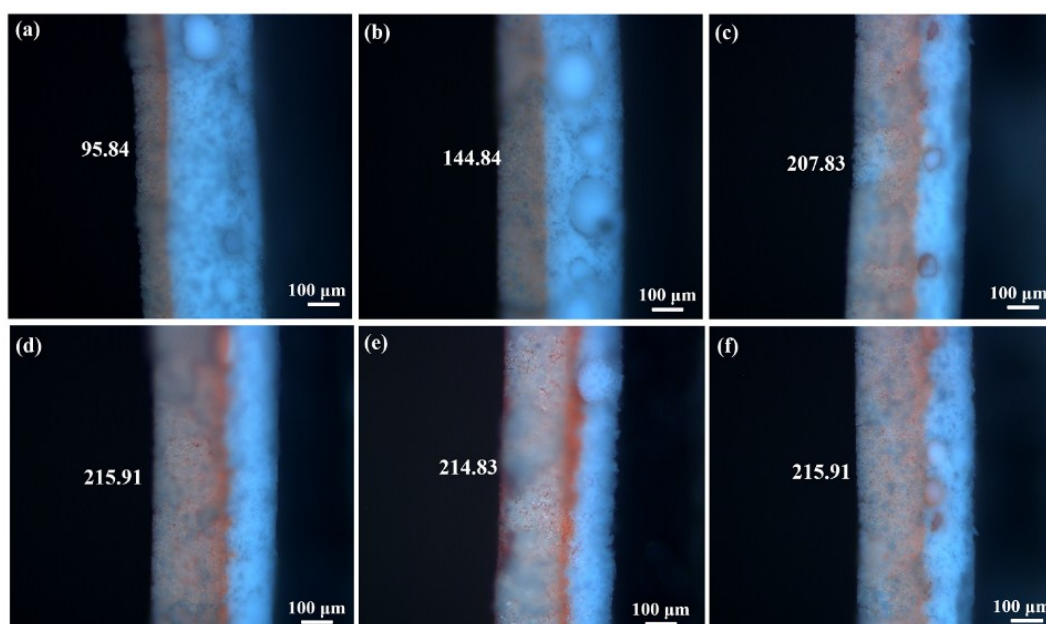


**Figure S5** The relationship between the thickness of hydrophilic layer and the immersion time in the mixed coagulation bath. (a-f): 1, 2, 3, 4, 5 and 6 min.

It can be seen from **Figure S6** that, when the AuNPs solution permeated heterostructured membrane from hydrophilic side to hydrophobic side (M-T) via gravity filtration, AuNPs were mainly embedded on the hydrophilic side to form a deep purple top surface and white bottom surface. In contrast, the AuNPs were embedded on the hydrophobic side when AuNPs solution permeated the membrane from hydrophobic side to hydrophilic side (M-B). The color for the hydrophilic side of membrane in which AuNPs permeated from hydrophobic side to hydrophilic side as shown in **Figure S6b** was darker than the hydrophobic side in **Figure S6a**. The reason may be that the hydrophilic surface is easier to absorb AuNPs than hydrophobic surface even though the hydrophobic materials have enough micro-/nano-structures.<sup>2</sup> Due to the existence of little amount of AuNPs on the opposite surface for M-B, the surface temperature (48.9 °C, **Figure 6c**) is higher than that of M-T (39.5 °C, **Figure 6c**).

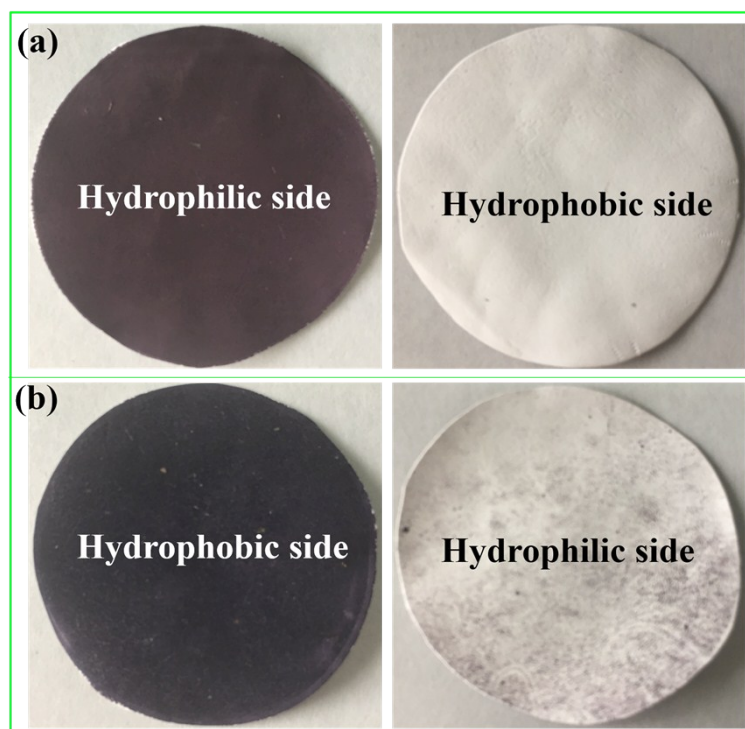


**Figure S6.** The images of heterostructured membrane-based absorbers. (a) AuNPs was loaded from hydrophilic side to hydrophobic side, the membrane was named M-T. (b) AuNPs was loaded from hydrophobic side to hydrophilic side, the membrane was named M-B.

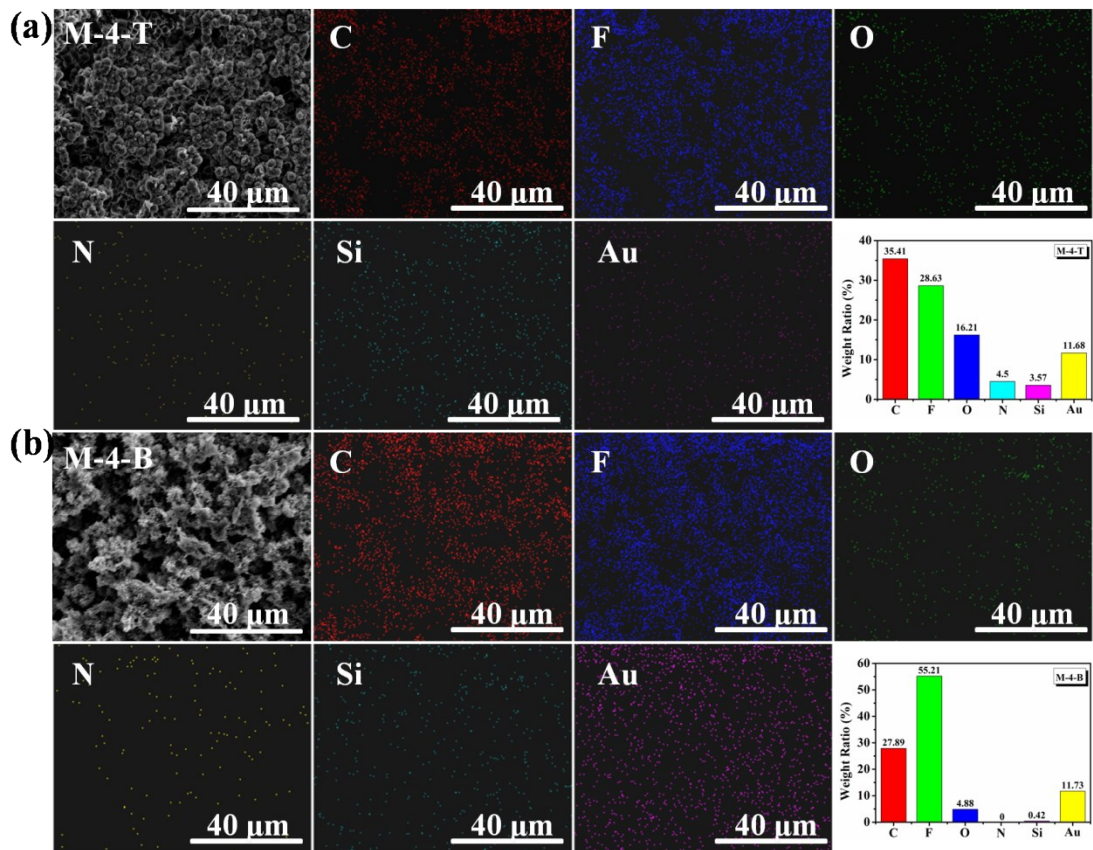


**Figure S7.** SEM images, EDS scanning images and element weight ratio measured by EDS for M-4-T (a) and M-4-B (b) after loading AuNPs respectively.

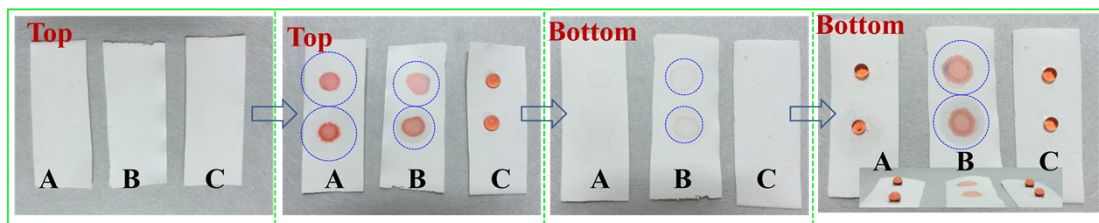


**Figure S8.** Wettability of top and bottom surfaces for heterostructured membrane A, hydrophilic membrane B and hydrophobic membrane C. Heterostructured membrane A shows hydrophilic top surface and hydrophobic bottom surface, both top and bottom surfaces of hydrophilic membrane B were spontaneously wetted, both top and bottom surfaces of hydrophobic membrane C kept water repellent. Both hydrophilic membrane and hydrophobic membrane shows symmetric wettability, while heterostructured membrane shows opposite wettability (water dyed with Congo Red).

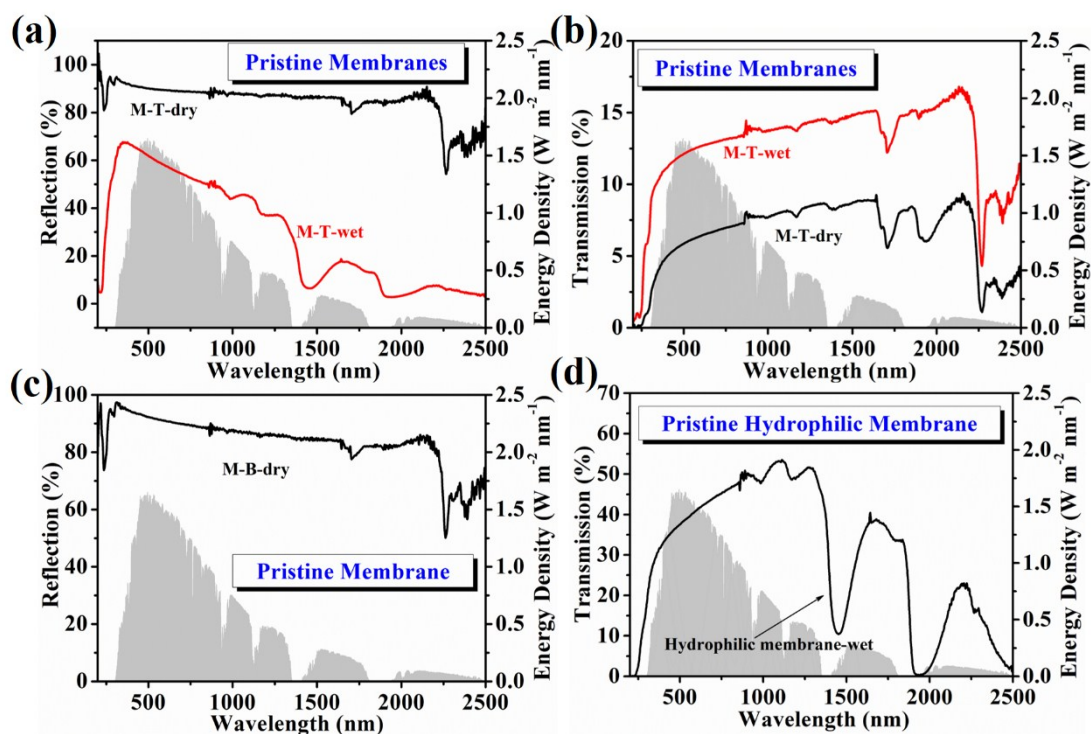


**Figure S9.** Reflection (a) and transmission (b) spectra of the pristine M-T membrane at dry and wet state respectively in the wavelength range of 200~2500 nm; (C) Reflection of pristine M-B; (d) Transmission of pristine hydrophilic membrane at wet state.

In order to illustrate the importance of roughness surface with micro/nano structure, we all fabricated the hydrophilic membrane with flat surface as shown in **Figure S10(a, b and c)**. The AuNPs was loaded on this surface by vacuum filtration. It can be seen from the insets in **Figure S10d**, the membrane showed a strong reflectivity no matter under dry state or wet state and the reflectivity for them was also detected using UV-vis-NIR spectrophotometer. The absorbance ability of the membrane, which was calculated from reflection and transmission spectra ( $A=100\%-R-T$ ), was lower than the membrane with micro/nano structure.

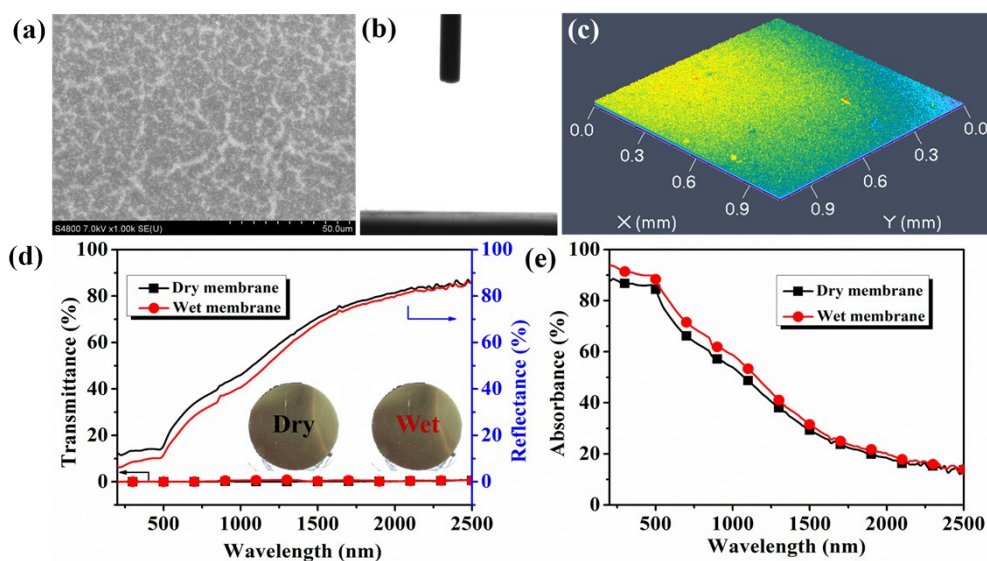


**Figure S10.** (a) SEM image of the flat surface; (b) The water contact angle of the flat surface; (c) 3D confocal microscope image of the flat surface; (d) Reflection and transmission spectra of the flat membrane with AuNPs at dry and wet state respectively in the wavelength range of 200~2500 nm; (e) The absorption of heterostructured membrane with AuNPs at dry and wet state respectively.

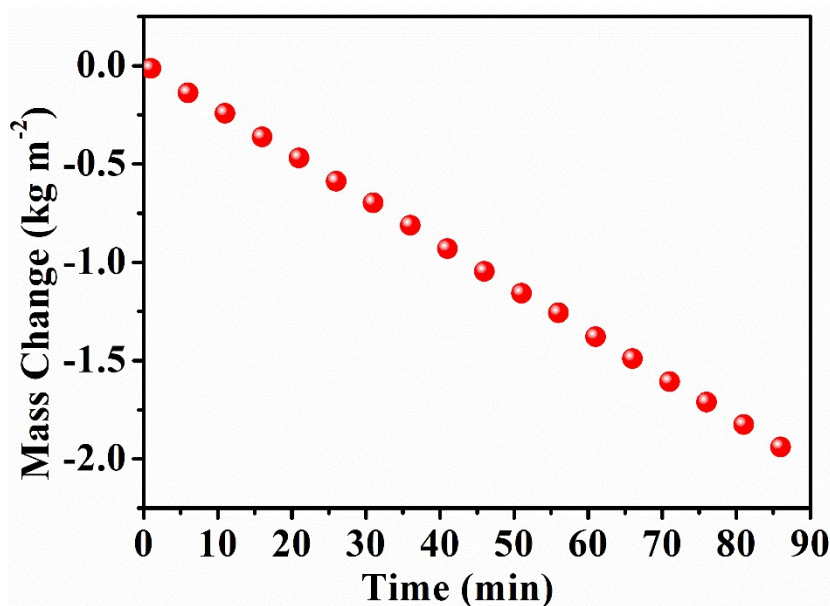


**Figure S11.** Mass change of salt water for hydrophilic membrane with AuNPs putted on PS foam. The PS foam was covered by cotton fiber to pump water. The measured evaporation rate and efficiency were  $1.35 \text{ kg m}^{-2} \text{ h}^{-1}$  and  $\sim 85\%$  respectively. The calculated conduction heat loss according to Equation S3 was about 3% when underneath bulk water increased by  $0.9 \text{ }^\circ\text{C}$ .

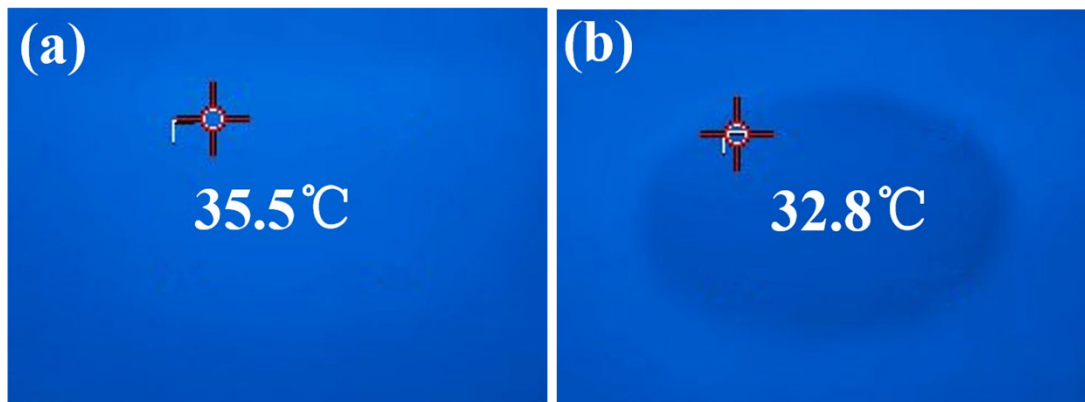


**Figure S12.** The surface temperature for PS foam and pure PVDF membrane under one sun illumination. PVDF membrane shows a lower thermal conductivity, indicating its superior heat insulation.

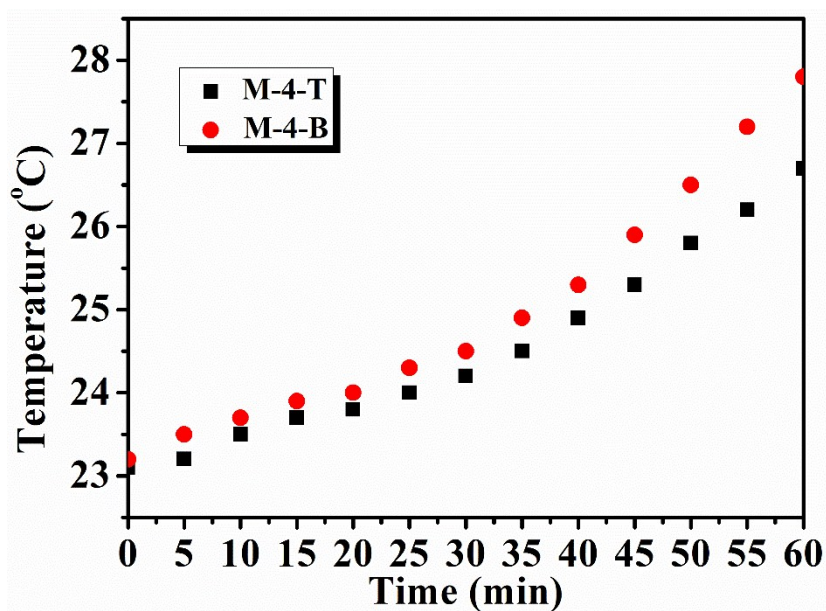


**Figure S13.** Changes of underwater temperature for M-4-T and M-4-B.

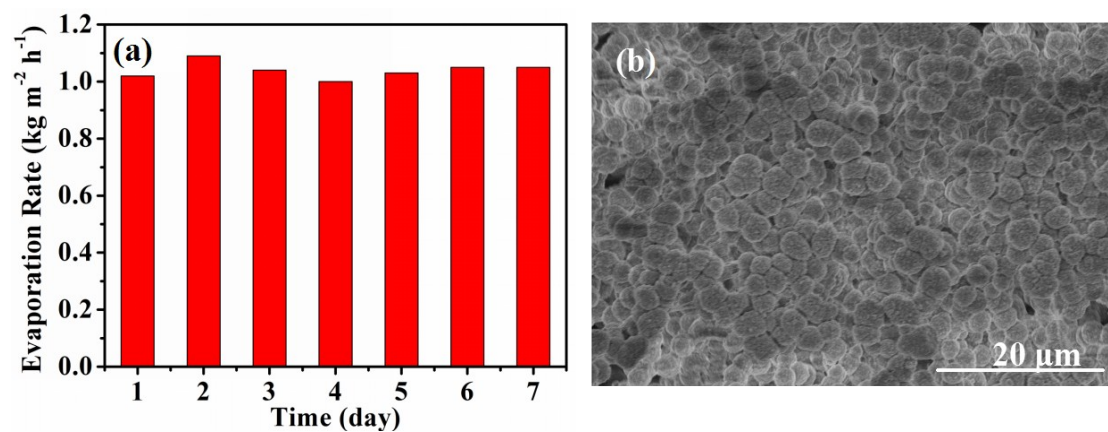


**Figure S14.** (a) The stability of M-4-T under 1 sun illumination after a certain period and the daily irradiation duration is 1 hour. (b) The heterostructured membrane structure after repeated measurement. It should be noted that the membrane used in this experiment was the one used in Figure 5g.

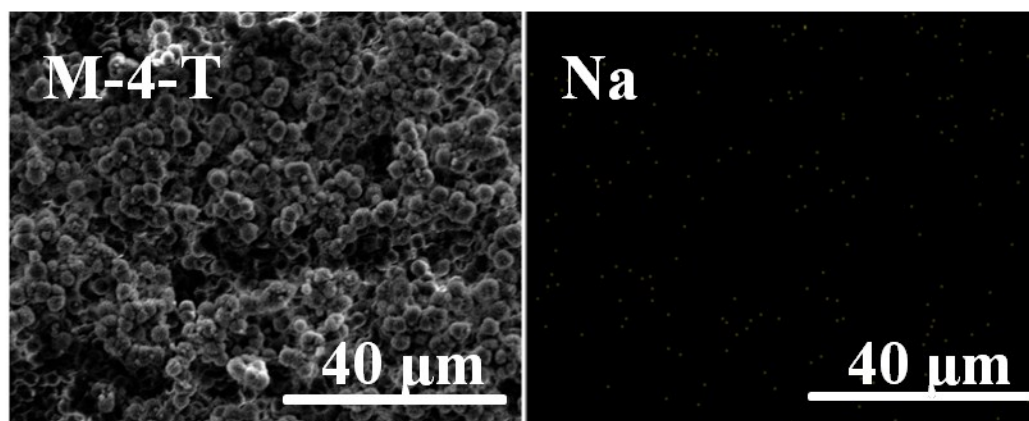


**Figure S15.** EDS scanning images exhibited the Na element distributions on membrane surface.

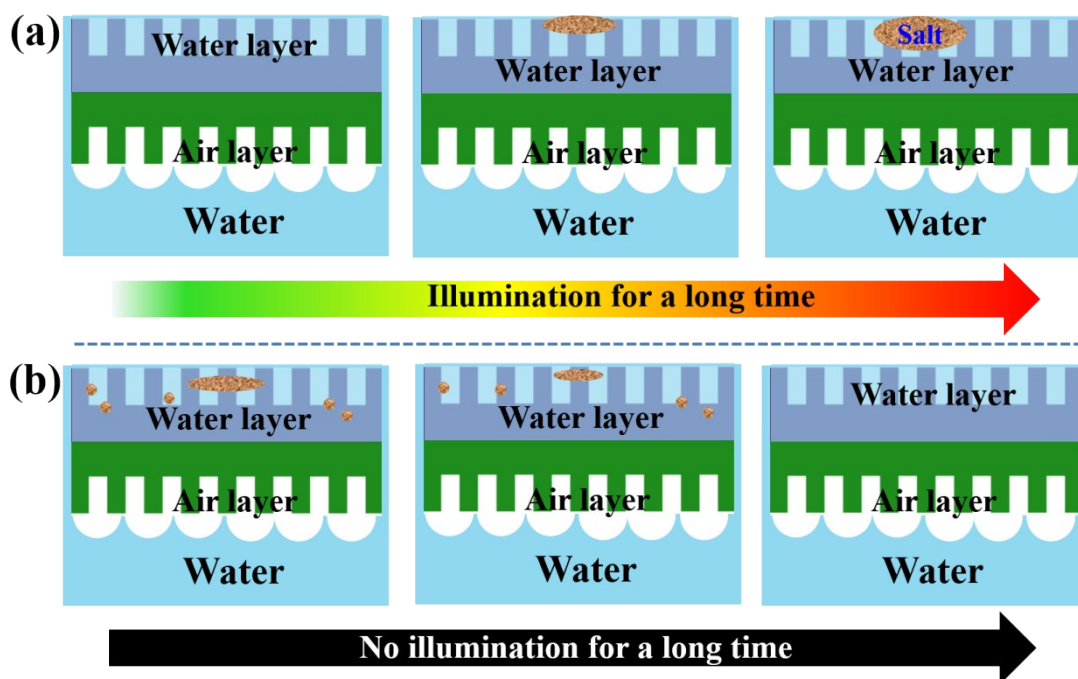


**Figure S16.** A schematic diagram for salt precipitation (a) and re-dissolution (b).

It can be seen from **Table 1** that the evaporation rate under 1 sun illumination in this manuscript is comparable to that reported in other literatures. When replacing AuNPs with carbon black nanoparticles, the evaporation rate can reach  $1.23 \text{ kg m}^{-2} \text{ h}^{-1}$  as exhibited in **Figure S17**.

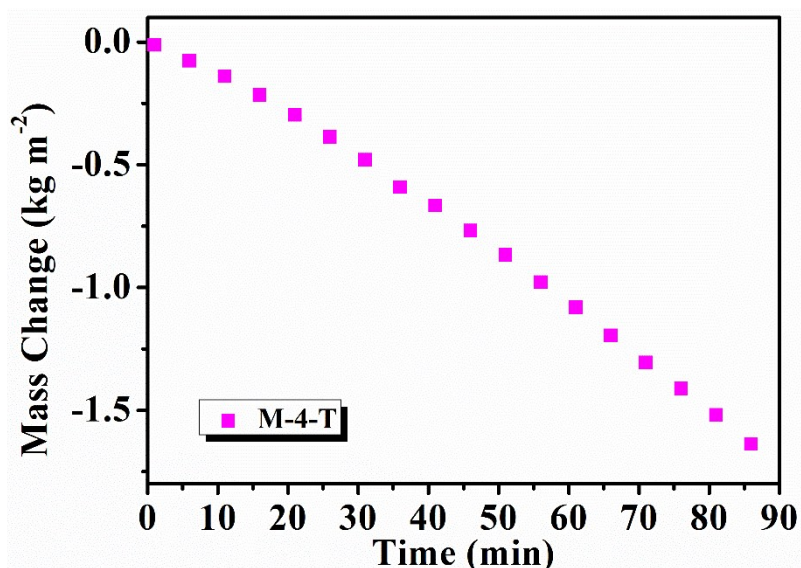


**Figure S17.** The relationship between mass change and time for M-4-T loaded with carbon black nanoparticles (CB). CB was loaded on the surface of the membrane by filtration.

## The analysis of heat loss:

(1) Radiation:

The radiation loss was calculated using the Stefan-Boltzmann equation:

$$\phi = \varepsilon A \sigma (T_1^4 - T_2^4) \quad (\text{Equation S1})$$

where  $\phi$  represents heat flux,  $\varepsilon$  is the emissivity, and emissivity in this equation is supposed has a maximum emissivity of 1.  $A$  is the surface area ( $\text{m}^2$ ),  $\sigma$  is the Stefan-Boltzmann constant ( $5.67 \times 10^{-8} \text{ W m}^{-2} \text{ K}^{-4}$ ),  $T_1$  is the surface temperature ( $\sim 36 \text{ }^\circ\text{C}$ ) of heterostructured membrane-based absorber at a steady state condition, and  $T_2$  is the ambient temperature ( $\sim 28 \text{ }^\circ\text{C}$ ) upward the absorber. According to the equation, the radiation heat loss is calculated  $\sim 5\%$ .

(2) Convection:

The convective heat loss is defined by Newton' law of cooling:

$$Q = hA\Delta T \quad (\text{Equation S2})$$

where  $Q$  represents the heat energy,  $h$  is the convection heat transfer coefficient ( $10 \text{ W m}^{-2} \text{ K}$ ), and  $\Delta T$  ( $\sim 8 \text{ }^\circ\text{C}$ ) is different value between the surface temperature of heterostructured membrane-based absorber and the ambient temperature upward the absorber. According to the equation, the connection heat loss is measured  $\sim 8\%$ .

(3) Conduction:

$$Q = Cm\Delta T \quad (\text{Equation S3})$$

where  $Q$  is the heat energy,  $C$  is the specific heat capacity of water ( $4.2 \text{ kJ }^\circ\text{C}^{-1} \text{ kg}^{-1}$ ),  $m$  ( $40 \text{ g}$ ) is the weight of pure water used in this experiment.  $\Delta T$  is the temperature difference of pure water after and before solar illumination under 1 sun after 1 h. The conduction loss are calculated  $\sim 13.4\%$  for M-4-T and  $\sim 17.0\%$  for M-4-B.

## References

1. S. Li, Z. Cui, L. Zhang, B. He and J. Li, *J. Membr. Sci.*, 2016, **513**, 1-11.
2. J. Lee, T. Laoui and R. Karnik, *Nat. Nanotechnol.*, 2014, **9**, 317-323.